Benefits of Non-Destructive Evaluation and Probabilistic Damage Tolerance Cosimulation for Fracture Risk Reduction

Fabrice Foucher[1], Sebastien Lonné[1], Philippe Dubois[1],
Stephane Leberre[2], Pierre Calmon[2], Michael Enright[3], Yasin Zaman[3]

[1] EXTENDE, Massy, France, contact@extende.com
[2] CEA DISC, Gif Sur Yvette, France
[3] Southwest Research Institute, San Antonio, TX, USA

Abstract

In the context of the damage tolerance approach used to drive aircraft maintenance operations, it is essential to demonstrate the reliability of NDE inspections in detecting structural damage especially for additively manufactured components since this process produces components that may introduce material anomalies at any location within a component. The Probability Of Detection curve (POD) that links the probability to detect a detrimental flaw to its size is generally used as a key indicator for that purpose by giving the maximum flaw size that a NDE process can miss with a given level of probability and confidence. This information can then be used along with other inputs such as component geometries, mechanical properties, constraints, service and residual stresses and damage evolution speed to assess fracture risk and then adapt maintenance scenarios to optimize safety and component service life.

NDE reliability and risk assessment are based on statistical indicators that need a large amount of data to provide reliable metrics. It is difficult to obtain such indicators using a purely empirical approach that is based on physical trials and measurements as it may involve many mock-ups and costly processes. Simulation tools can achieve this goal via their ability to include and precisely monitor many parameters as well as high computing capacities that are now available.

The work presented in this paper involves cosimulations performed between the DARWIN® probabilistic damage tolerance software and the CIVA NDE modelling software and connects together NDE and Fracture mechanics simulations, two disciplines that generally work on their own. DARWIN computes fracture risk levels throughout a component, while CIVA can efficiently provide Probability Of Detection curves at different locations in a component and for various NDE methods. The presented application deals with a titanium gas turbine engine impeller disk and involves an Ultrasonic NDE inspection technique.

1. Introduction

Non-Destructive Evaluation (NDE) can be used to detect detrimental flaws that may influence the structural integrity of a component. To be effective, NDE cannot operate "alone". Indeed, the critical flaw sizes and their characteristics (location, profiles, etc.) should be based on a sound basis, whether it be past observations and above all, mechanical data and fracture mechanics considerations. The sizes of the critical flaws can have a direct influence on the development of the NDE method. On the other hand, NDE can provide relevant metrics to establish efficient maintenance strategies. The damage tolerance approach that is used to develop aircraft maintenance operations is an example of such a strategy where the detection performance of the NDE, along with other information, is used to define appropriate maintenance & inspection cycles. In this context, NDE and fracture mechanics need to work together.

The performance of NDE is often estimated with an indicator called "Probability of Detection" (POD) that links the probability to detect a detrimental flaw to its size. To be useful, this statistical indicator must be based on relevant and quite large data sets, to provide "an acceptable confidence" on the results and be representative of the variability of the inspection conditions and situations that may occur in the field. As a component is generally made of different characteristic areas in terms of geometric features, thicknesses, stresses or other properties, which is especially the case with new manufacturing techniques such as additive manufacturing, an efficient risk

assessment may require more than a single POD curve to quantify the risk at various regions (i.e., zones) within a component. This implies that even more data may be required to quantify multiple POD curves that may be associated with the risk assessment of a component.

It is often very difficult and costly to obtain enough relevant data based on a single set of experimental results. NDE numerical simulation tools can be particularly useful at that stage thanks to their ability to generate a very large amount of data at a relatively low cost. Probabilistic damage tolerance (PDT) enables the prediction of fracture risk in different zones of a component and assuming different hypotheses in terms of flaw types, flaw prevalence and NDE performance.

This article illustrates the joint use of NDE and PDT numerical simulations for the fracture risk assessment of a titanium gas turbine engine component.

2. Modelling tools for NDE and Probabilistic Fracture Mechanics

2.1 Use of CIVA modelling platform for NDE and POD simulation

NDE inspection simulation has been performed using the CIVA software, a platform developed by the French Atomic Energy Commission "CEA" dedicated to NDE and distributed by EXTENDE. The various modules of CIVA provide access to different NDT methods and techniques: Ultrasonic Testing (UT), Guided Waves Testing (GWT), Eddy Current Testing (ET), Thermographic Testing (TT), Radiographic Testing (RT) & Radiographic Computed Tomography (CT). The mathematical formulations used in the different modules often rely on semi-analytical models which approach provides support for a wide range of applications while offering very competitive calculation times. To continue the extension of the application fields of CIVA, it is sometimes necessary to rely on more general numerical approaches (FEM, Finite Difference, etc.). To keep the benefits of the semi-analytical strategy, the current trend within CIVA is to build hybrid models, a part of the computation being done by fast semi-analytical models, another part being completed by numerical approach when necessary for the validity of the results. For interested readers wishing to have more information on the models, the following reference papers are available [1], [2] and [3] for the Ultrasonic tool used in this study. CIVA also includes metamodels which are particularly useful in the frame of a reliability study. A metamodel is a surrogate model relying on "smart interpolators" and is built to replace a physical-based model. The first step consists of computing a database of simulation results for a given range of parameter variations. The metamodel is built from these reference data and, after having evaluated its accuracy, it enables a real-time exploration of the full range of inspection scenarios constituted by the full variation of parameters. It provides the possibility to perform a statistical analysis of the simulated data that is required for sensitivity and POD studies.

2.2 Introduction to DARWIN software and Probabilistic Damage Tolerance approach

DARWIN® ("Design Assessment of Reliability With Inspection") is a software program developed by Southwest Research Institute® (SwRI®), based in San Antonio, Texas, USA. DARWIN enables the computation of fracture risk with and without the influence of non-destructive inspections using NDE and mechanical parameters as inputs. More precisely (see Fig. 1), the input variables for DARWIN include component stress results from finite element (FE) models (standard FE model results such as ANSYS and ABAQUS are supported), material stress-strain and fatigue crack growth (FCG) rate properties, anomaly (i.e., flaw or defect) distributions, inspection schedules, and location-specific POD curves (among others).

To compute risk, DARWIN discretizes the component into a number of zones that can have different material properties, types of anomalies, service and residual stresses. DARWIN also includes the capability to compute critical initial crack sizes (CICS) at selected locations within a FE component model. The CICS is the initial flaw size that will just grow to failure within the service life of the component at a given location. The CICS also represents the smallest flaw size that needs to be detected by NDE (smaller flaws do not grow to failure and therefore do not need to be detected). The CICS approach provides key inputs that are necessary for NDE inspection design (i.e., the target flaw sizes that need to be detected at various locations). Based on this, NDE simulation can be used to design and simulate the inspection technique and provide the corresponding POD curves per zone to DARWIN that will then estimate risk per zone as a function of component cycles of usage. From that information, NDE can adapt either the level of performance of the NDE or the rate of inspections to

find a cost-effective solution and lower the fracture risk, which, illustrates the virtuous cycle of the PDT approach. Further information regarding DARWIN is provided in References [4-8].
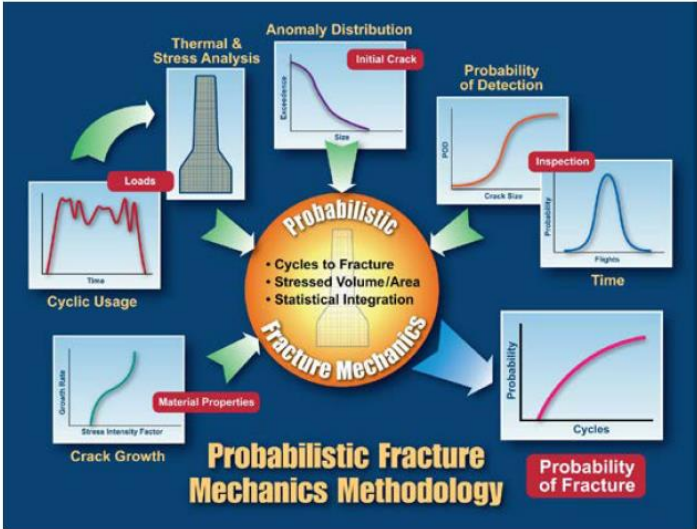

Figure 1. Overview of Probabilistic Damage Tolerance approach with DARWIN

3. Application case

Compared to traditional manufacturing processes, the application of additive manufacturing techniques can lead to significant reductions in component fabrication costs. However, it can also introduce new anomaly types in large numbers such as pores or lack of fusion between powder particles. Some of these defects, present at the manufacturing stage, can lead to larger and critical cracks if they are located in a region of high cyclic stress. The present works deals with a turbine engine titanium component for the aerospace industry. The geometry of the component is visible on Figure 2, it measures about 275 mm in diameter and 120mm in height.
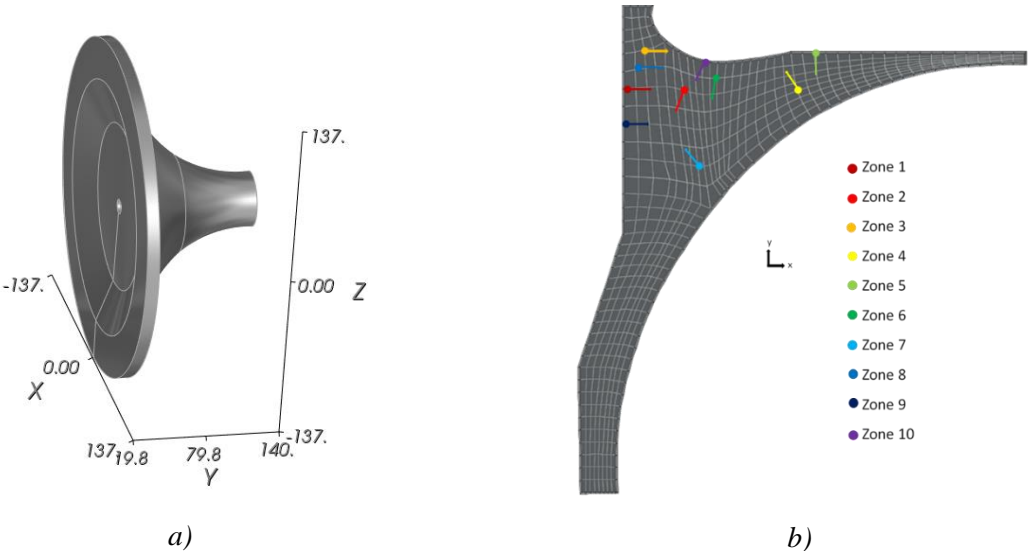

a)   b)

Figure 2. a) Titanium rotor geometry and overall dimensions
b) Discretized cross section by DARWIN and selection of 10 flaw areas.

Having processed a first set of mechanical properties, DARWIN can discretize the cross section of a component into different zones that can likely have different fracture risk values, as in the example shown in Figure 2b. The number of zones to investigate in terms of NDE may not be that extensive. Indeed, when a sufficient number of zones are considered, adding more zones does not substantially improve the accuracy of the overall risk assessment. In this study, aimed at illustrating the NDE-PDT cosimulations concept, only ten zones have been selected, corresponding to the ten arrows displayed on Figure 2b.

Two types of flaws have been considered in these zones:
- Planar circular defects orientated in the radial section of the rotor, representative of cracks growing during the service life,
- Spherical anomalies, already present at the manufacturing stage.

All cracks grow in the component radial plane, and arrows on figure 2 indicate primary crack growth directions.

The CICS values are displayed in Table 1. The 10 flaws located in the component model in CIVA are illustrated on Figure 3. Flat Bottom Holes have been used for this purpose. This image illustrates well the variety of flaw critical sizes depending on the considered zone.

Table 1. CICS values computed by DARWIN

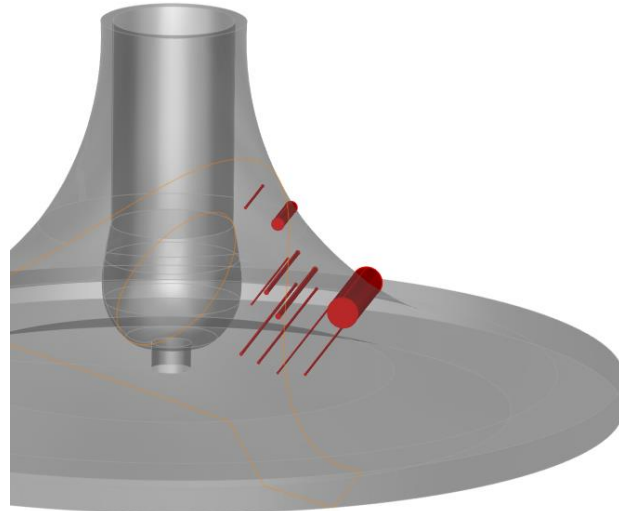| Zone ID	CICS radius	
	(in)	(mm)
1	0.0118	0.2984
2	0.0315	0.7998
3	0.0183	0.4650
4	0.0754	1.9153
5	0.0156	0.3961
6	0.0254	0.6440
7	0.1859	4.7219
8	0.0161	0.4079
9	0.0141	0.3573
10	0.0121	0.3063

Figure 3: Illustration of the 10 flaws in the CIVA 3D model.

4. NDE modelling and POD study

4.1 Description of the UT inspection technique

Before being able to compute POD curves, it was necessary to define one or several relevant inspection techniques. The UT method was targeted. At first, the crack cases were investigated. Considering flaw orientations along the radial section, the inspection from the flat end of the component looked very unpromising and therefore an inspection strategy based on an immersion technique applied from the toric side of the impeller was considered. It assumes that a mechanized holder be set to position and orientate the probe in a relevant way for the inspected zones. Then, a rotating arm would allow to cover the whole circumference of the component.

The probe is made of 64 elements with a pitch of 0.3mm and has a 10 MHz centre frequency. 32 elements are enabled in the same group to adjust the active aperture. Both sector and electronic scans are then performed to cover a quite large zone in the component section with shear waves. Authors would like to mention here that this inspection technique was designed for demonstration purpose and does not represent a finalized solution. Optimization works, hardware and robotic implementation would be necessary to assess its fitness for such inspection. In Figure 4, the inspection concept and the sound beam propagation for one refraction angle is illustrated (CIVA simulation result) for an area covering the zones #6 and #10, initially defined by DARWIN. The ultrasound focal spot looks well orientated and located in the component. The covered area in a section including all angles and groups of firing elements (for this zone) is also represented on Figure 5 thanks to a sensitivity coverage simulation (that also takes into account the target defect orientation).
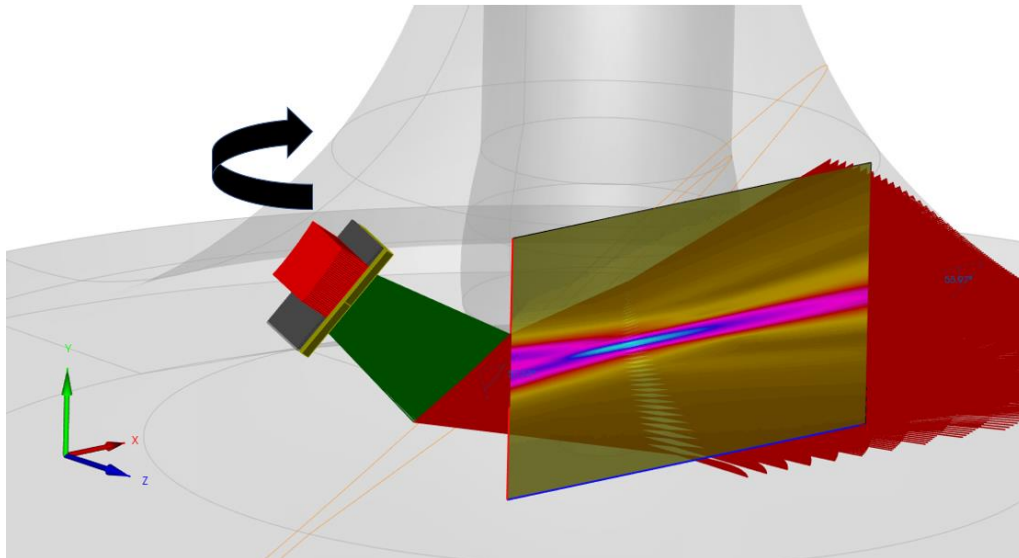
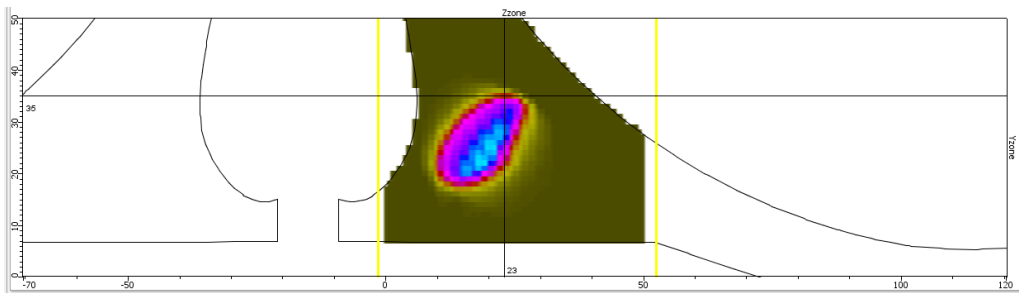*Figure 4: Shear waves Sound beam propagation simulation in zone #6.*

Figure 5: Sensitivity coverage simulation for zone #6 and zone #10.

In Figure 6, the simulation of the crack response with this probe in zone #10 is illustrated. The Flat Bottom Hole used here to model this type of defect is represented at its CICS size, i.e., 0.6mm diameter. The maximum amplitude obtained here has been evaluated to -2.4dB compared to one 0.5mm diameter FBH located in a planar component made of the same material and considering a specular reflection of the beam on this reference flaw, which appears to be a pretty good level of sensitivity for a first approach.
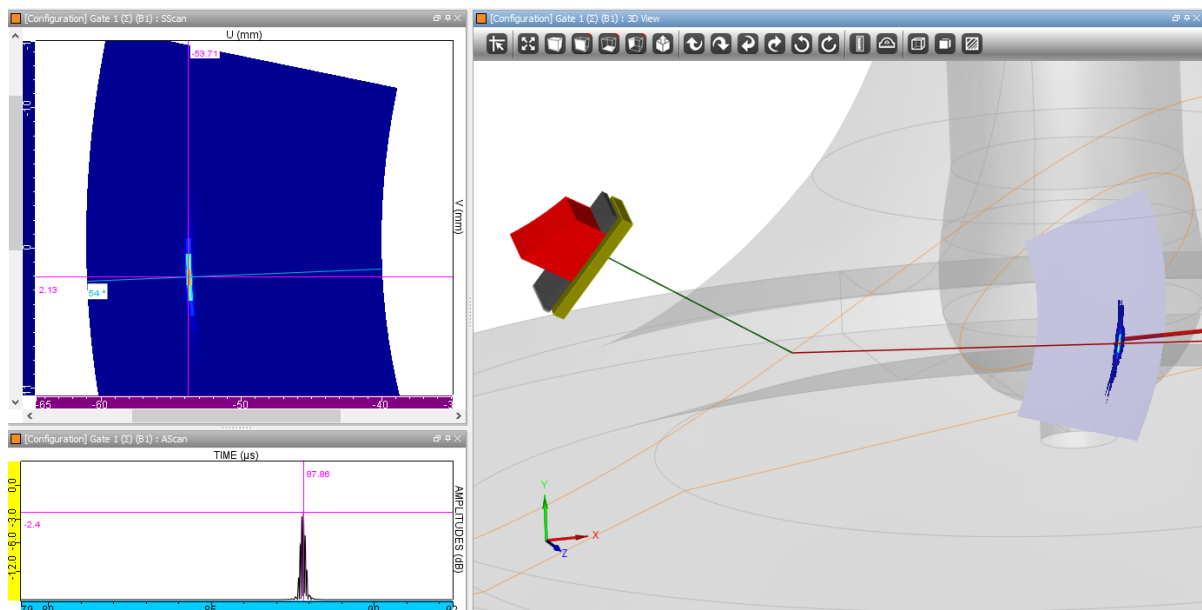

*Figure 6: Defect #10 inspection simulation.*

4.2 Sensitivity analysis

Calculating POD curves means estimating the reliability of an inspection method considering the variability of uncertain and influential parameters for different flaw sizes. Uncertain parameters can include flaw parameters (size, orientation, location, etc.), component uncertainties (geometry, physical properties), inspection parameters (probe parameters, positioning or scanning variability), or environmental and human factors. From a MAPOD (Model Assisted POD) point of view, this assumes introducing relevant variable parameters in the model and propagating the uncertainties by sampling the data and simulating the different situations. The choice of uncertain parameters is not obvious and requires discussions with experts and/or preliminary investigations with the model. Interested readers may refer to the following references for more information regarding the required methodology for MAPOD studies and methodology ([9], [10], [11]). In this project, the following variable parameters have been selected:

- Flaw size (diameter),
- Ultrasound wave velocity in the component (+/- 300 m/s around the nominal mean value)
- Flaw orientation (+/-10° around its nominal orientation),
- Probe position on the component (+/-2mm around the nominal one),
- Probe deflection angle (+/-1.5° around the nominal angle).

An adapted range of variation have been defined for each parameter from which a multiparametric design of experiment has been performed based on a Latin Hypercube Sampling technique. To enable exploration of various inspection scenarios in post-processing without having to launch new simulations, the strategy was to build a metamodel from this simulation database, rather than relying on a fixed data set. The metamodel is automatically generated in CIVA for each parametric study. Figure 7 illustrates this metamodel performed for the inspection simulation of the target flaw #10. It includes the visualization on a parallel plot of the 1500 simulations performed (each parameter is plotted on different columns and the results obtained are on the right column, here the maximum UT signal amplitude), the assessment of the metamodel accuracy vs the reference simulation ("True vs Predicted" graph) , then the use of the metamodel to evaluate impact of influential parameters and finally parameters' impact ranking thanks to Sobol indices (flaw size and flaw skew are for instance the predominant parameters in this case). The strength of metamodels is that any different combination of parameters (i.e., inspection scenarios) or any different density functions representing their likelihood can be tested and provide new results in real time.
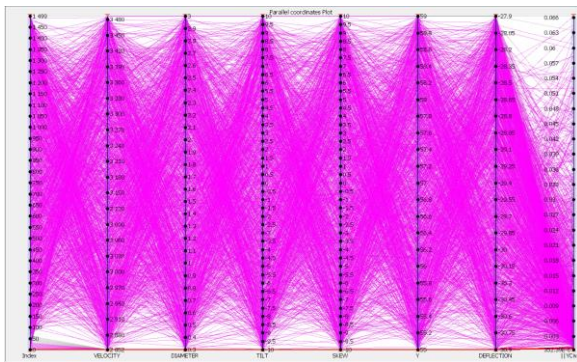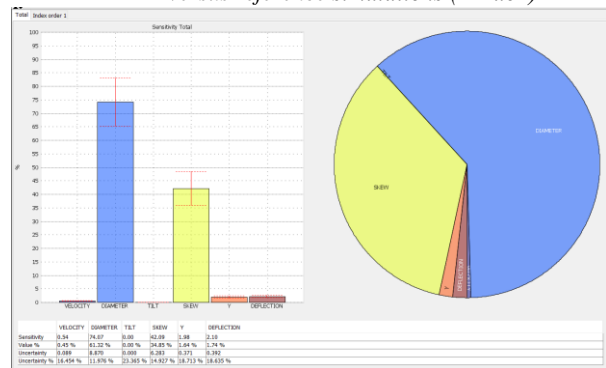

a) *Parallel plot illustrating the simulated design of experiment*
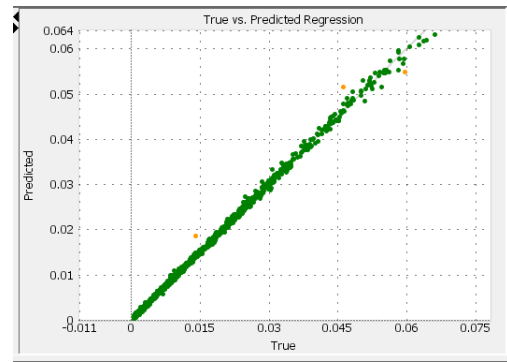
b) *Metamodel accuracy estimation ("Predicted") versus reference simulations ("True")*
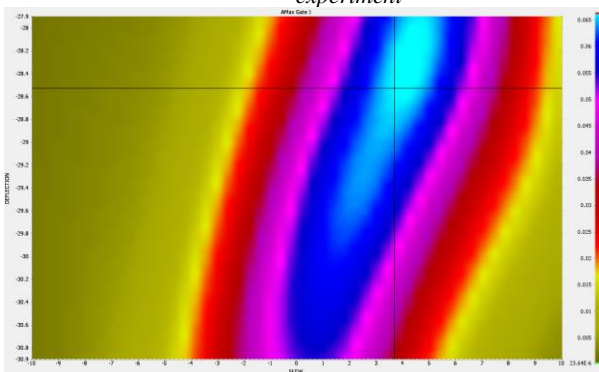
c) *Impact on probe deflection and defect orientation on UT signal strength using metamodel*

d) *Sobol indices ranking the shared influence of the variable parameters*

Figure 7: Sensitivity analysis outcomes in CIVA for target flaw #10.

4.3 POD Curves

The generation of POD curves consists of extracting datasets from the metamodel for the given density functions assumed for the uncertain parameters and for different flaw sizes. Results (signal amplitudes here) are placed on the Y-axis and flaw size is on the X-axis (â vs a plots). From these plots, different POD analysis techniques can be performed in CIVA, including the standard parametric approaches "Signal Response" or "Hit-Miss", generally adopted by the aircraft industry and described in the Military Handbook 1823A [12]. Again, many different scenarios can be tested here in real time thanks the metamodel, without having to launch new simulations.

For instance, a POD curve obtained on Flaw #10 is displayed in Figure 8. The inspection scenario assumes 17 different flaw sizes with diameters ranging from 0.3 to 0.7mm. 50 inspections per flaw size were considered accounting for different probability density laws for the uncertain parameters (normal law around their nominal values with a standard deviation of 10% of their variation ranges mentioned in the previous paragraph). Decision thresholds have been set at -6dB compared to the amplitude of a reference specular echo obtained on a Flat Bottom Hole located in a planar block made of the same material. The diameter of the reference FBH reflectors are adapted to the target flaw size (a 0.5mm diameter was selected for flaw #10). These decision thresholds assume that there is a good enough SNR to distinguish signals from the background noise at this amplitude level, which appears to be a likely assumption but should be confirmed experimentally. Finally, these POD curves are exported in ASCII-formatted data files that can be read by DARWIN. The probability of detection of 90% with 95% confidence, the "famous" $a_{90/95}$, is reached for a flaw diameter of 0.5mm, that is 0.25mm radius, below the CICS value provided by DARWIN, for zone #10.
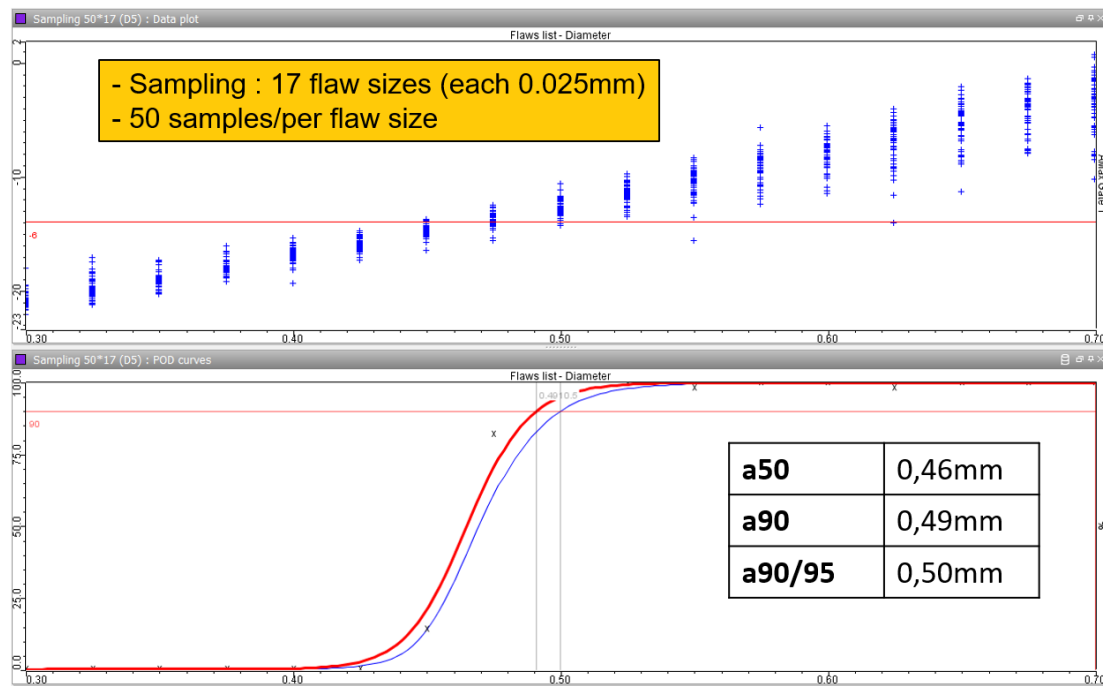

Figure 8: POD curves simulated with CIVA for target flaw #10.

5. Fracture Risk Assessment

Figure 9 shows all POD curves imported from CIVA to DARWIN for the 10 crack locations and another POD curve called "FAA AC 33.14-1" that was used as a reference (US Federal Aviation Administration Advisory Circular 33.14-1 [13] includes a set of reference POD curves for the aircraft industry). The "FAA AC 33.14-1" curve shown in Figure 9 is a UT inspection POD curve that is based on a rejection threshold equivalent to a 1/64-inch (about 0.4mm) diameter Flat Bottom Hole.

Once all POD curves are transferred to DARWIN, the tool can compile this data along with information regarding defect prevalence and other fatigue crack growth-related information to compute fracture risk (i.e., probability of fracture or failure) curves versus usage (flight) cycles of the component. The fracture risk here

corresponds to the "unconditional risk", that is, the risk level without prior knowledge of the presence or absence of a defect. Risk curves are computed for each of the following cases:

- No inspection at all,
- Inspection at manufacturing stage with a NDE performance characterized by 2 different POD curves:
    o FAA reference POD curve,
    o "CIVA simulated inspection" location specific POD curve,
- In service inspection performed after 10,000 cycles (again with NDE performance characterized by both POD curves mentioned above),
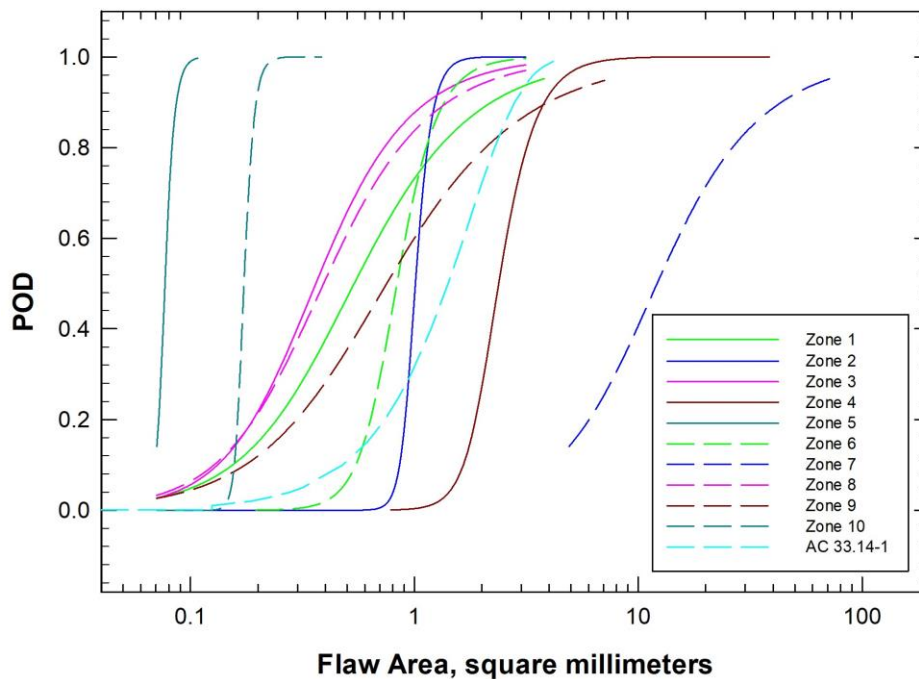- Inspection performed both at manufacturing and in service.

Figure 9: Eleven POD curves considered in DARWIN for planar cracks.

5.1 Zone 8 – Planar crack

In Figure 10, a first example of risk assessment is provided corresponding to zone 8. The highest curve in light green shows the increase of the risk level (i.e., probability of fracture or failure) with flight cycles without any inspection. If after 10,000 cycles NDE inspection is performed, the risk reduction is characterized by the pink curve if it is assumed that the inspection POD is characterized by the FAA curve. It can be observed that after 13,000 cycles, the risk increases again meaning that some smaller flaws which had not been rejected by the FAA NDE curve have then been growing to a more critical size.

Now, if the in-service inspection is performed by the NDE corresponding to the CIVA model, it leads to a better performance and a risk level that remains nearly constant until 20,000 cycles (see dark green curve).

Let us consider now that the inspection is applied at the manufacturing stage. The risk level is characterised by the light blue and the dark blue curves, respectively for the FAA and CIVA model POD curves. Risk is much more reduced in this case. Finally, if combining inspections at manufacturing and in-service (corresponding to the purple and dark blue curves), it can be observed that when the manufacturing inspection is performed with the CIVA model-based performance level, the in-service inspection provides no additional reduction in risk, whereas it is not the case with the FAA POD curve. In other words, the manufacturing inspection is so effective that it eliminates cracks that could be found during an in-service inspection at 10,000 cycles. If an in-service inspection is still desired, it could potentially be postponed to a later time when there may be larger cracks that can be found. These simulation tools could be used to identify the optimal timing of the in-service inspection in this scenario.
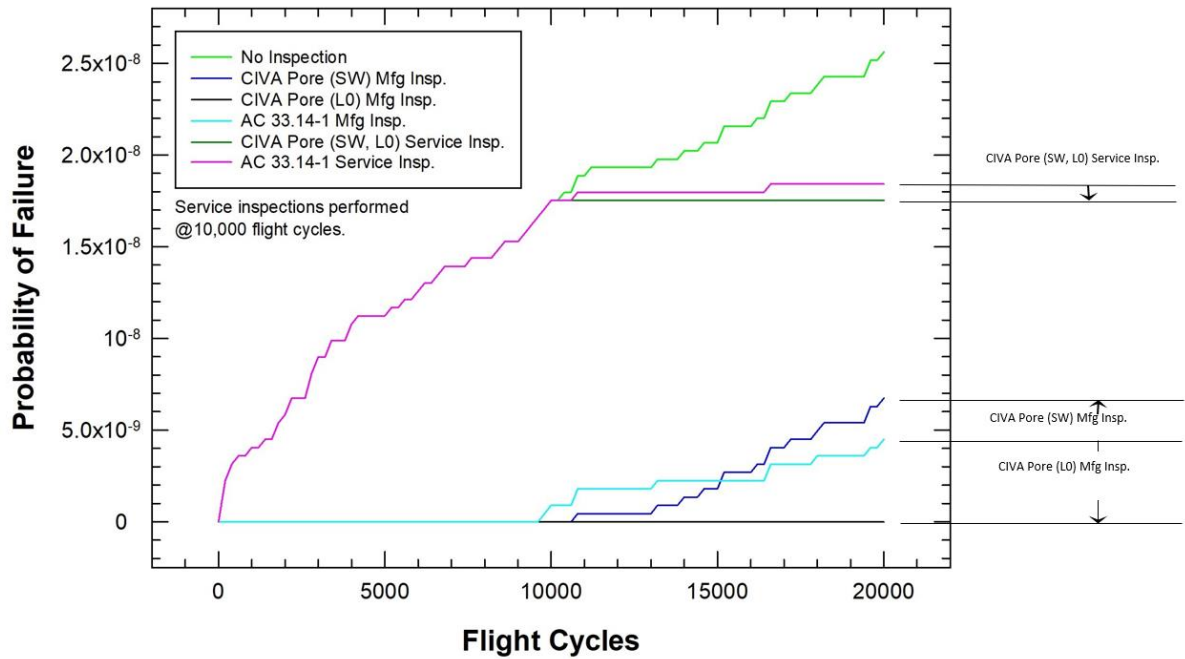
Figure 10: Risk assessment curves obtained by DARWIN for zone #8.

5.2 Zone 6 – Sphere

Another type of flaw considered in this study was spherical anomalies. Flaws in forged titanium materials are typically modelled as spheres [13]. Gas pores that are often present in additively manufactured components at the fabrication stage are also commonly modelled as spheres. At first, the same inspection method (based on shear waves) has been applied and simulated in CIVA leading to a quite poor NDE curve. Indeed, the S-waves method really aimed at generating a specular echo on a planar flaw in the radial section of the component. But for a spherical gas-pore, an inspection using straight beam with L-waves with a transducer located on the flat part of the specimen looks both much more efficient and easier to set up (illustrated on Fig. 11). This second inspection technique has then been simulated in CIVA from which a new POD curve has been calculated, showing a much better performance. The POD curves for zone 6 are displayed on Figure 12. It is also interesting to notice that the S-waves POD curve looks much less efficient than the FAA one for small flaw size but starts to reach a higher POD from a certain flaw size (around 3 square millimetres, that is around 1.9mm diameter).
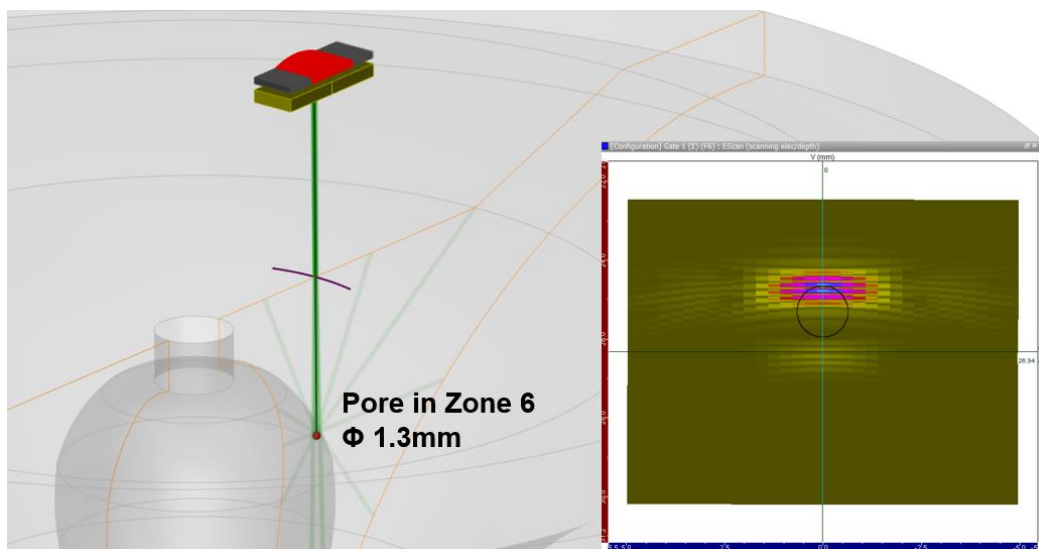

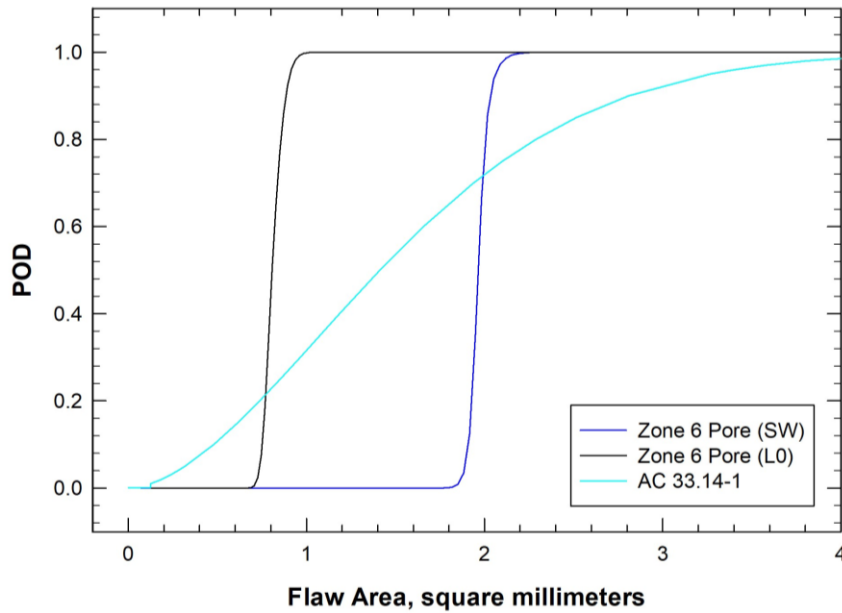*Figure 11: More suitable L0• technique for pore #6 simulated in CIVA*

Figure 12: POD curves for spherical pores on zone #6.

Considering the risk assessment curves (see Fig.13), it is interesting to compare the impact of both NDE techniques simulated in CIVA. Compared to the FAA curve, the risk reduction is lower with the S-waves inspection technique at the manufacturing stage. Indeed, as seen on POD curves, for small flaws the S-waves technique is not efficient enough. But for in-service inspection where the population of defects is expected to include larger flaws, the simulated S-waves method leads to a higher risk reduction than the reference FAA one. Now, if we look at the L0° method simulated for which the efficiency is much better for small flaws (a90/95 is reached for about 1mm diameter), the risk reduction is really strong even if the inspection takes place at the manufacturing stage. For this case, DARWIN helps to conclude that an adapted inspection method is necessary to achieve a significant risk reduction for spherical pores. Therefore, a unique technique based on shear waves cannot efficiently apply for all types of defects expected in this example component.
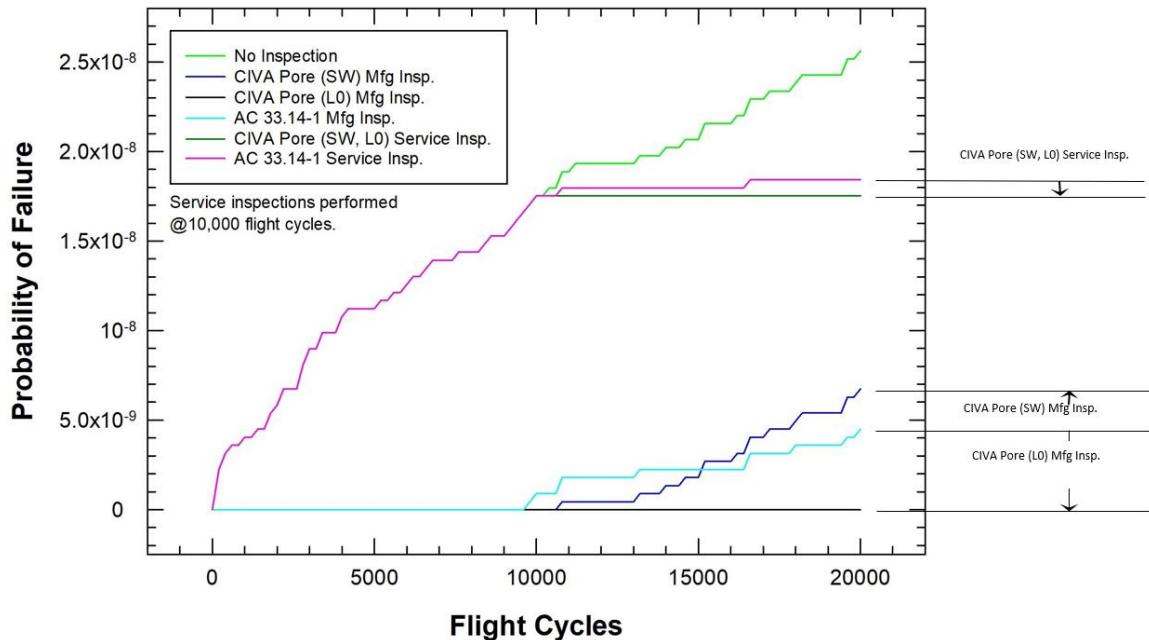

Figure 13: Risk assessment curves obtained by DARWIN for spherical pores in zone #6

Thanks to the combination of CIVA and DARWIN simulations, all zones could be investigated following the same methodology and for various hypotheses. At the end, synthetic risk assessment curves can be also built in DARWIN for the entire specimen to estimate an overall risk for its structural integrity.

6. Conclusions

This paper introduces a collaborative work performed by EXTENDE and SwRI based on cosimulations between CIVA and DARWIN software. CIVA helped to design inspection methods for the inspection of a titanium rotor component and computed location specific POD curves assuming some uncertain parameters in the inspection. DARWIN helped to define the different characteristic zones in terms of mechanical constraints and critical initial flaw sizes that allowed to initialize properly the CIVA models. Finally, the POD curves calculated by CIVA have been sent to DARWIN which can use them to predict the evolution of fracture risks in the component versus usage cycles, considering different hypotheses in terms of NDE performance and inspection planning. This cosimulations work illustrates the virtuous circle induced by a close collaboration between NDE and PDT staff. Even if the case described in this paper is an illustrative example and could deserve more work (optimization of the inspection technique, experimental verification of background noise and sensitivity levels, etc.), some promising conclusions can be asserted:

- NDE is useful for safety! NDE people are probably already convinced of that, but DARWIN quantifies this in terms of risk reduction,
- DARWIN computations help to determine detrimental flaw types, locations and sizes which are key inputs to develop an effective NDE inspection method,
- Simulations in CIVA enable engineers to produce at low cost a large amount of relevant data capable of building location-specific POD curves and not only one overall POD estimation, which gives much more insight for the fracture risk assessment of the component,
- The risk curves provided by DARWIN enable the engineer to adjust the level of effort to put on the NDE method, as illustrated on zone 8 for cracks and zone 6 for spherical pores in this paper, to find the best compromise between cost and efficiency, which can be summarized as cost-effectiveness.

Authors hope that this type of study can motivate future works and recommended practices for NDE and fracture mechanics based on such PDT methodology.

References

[1] S. Mahaut, S. Chatillon, M. Darmon, N. Leymarie and R. Raillon, 2009, *An overview of UT beam propagation* and flaw scattering models in CIVA, QNDE.

[2] M. Darmon, S. Chatillon, 2013, *Main Features of a Complete Ultrasonic Measurement Model: Formal Aspects of Modeling of Both Transducers Radiation and Ultrasonic Flaws Responses*, Open Journal of Acoustics, Vol.3 No.3A, http://file.scirp.org/Html/8-1610079_36873.htm#txtF2.

[3] A. Imperiale, E. Demaldent, "A macro-element strategy based upon spectral finite elements and mortar elements for transient wave propagation modeling. Application to ultrasonic testing of laminate composite materials", International Journal for Numerical Methods in Engineering, 2019;119:964–990. https://doi.org/10.1002/nme.6080

[4] M.P. Enright, R.C. McClung, J.C. Sobotka, J.P. Moody, J. McFarland, Y-D. Lee, I. Gray, and J. Gray, 2018, "Influences of non-destructive inspection simulation on fracture risk assessment of additively manufactured turbine engine components," paper GT2018-77058, Proceedings of the 63rd ASME International Gas Turbine & Aeroengine Technical Congress, Lillestrom, Norway, June 11-15, 2018.

[5] R.C. McClung, Y-D. Lee, J.C. Sobotka, J.P. Moody, V. Bhamidipati, M.P. Enright, D.B. Guseman, and C.B. Thomas, 2018, "Some recent advances in engineering fracture modeling for turbomachinery," Journal of Engineering for Gas Turbines and Power, ASME, 141 (2) pp 141(2): 021005.

[6] M.P. Enright, J.P. Moody, and J.C. Sobotka, 2016, "Optimal automated fracture risk assessment of 3D gas turbine engine components," paper GT2016-58091, Proceedings of the 61st ASME International Gas Turbine & Aeroengine Technical Congress, Seoul, South Korea, June 13-17, 2016.

[7] R.C. McClung, Y-D. Lee, M.P. Enright, and W. Liang, 2014, "New methods for automated fatigue crack growth and reliability analysis," Journal of Engineering for Gas Turbines and Power, ASME, 136 (6) pp. 062101:1-7.

[8] M.P. Enright and R.C. McClung, 2011, "A probabilistic framework for gas turbine engine materials with multiple types of anomalies," Journal of Engineering for Gas Turbines and Power, ASME, 133 (8) pp. 082502:1-10.

[9]   B. Chapuis, P. Calmon, F. Jenson, 2016, Best practices for the use of Simulation in POD Curves Estimation, IIW Collection, https://doi.org/10.1007/978-3-319-62659-8

[10]   F. Foucher et al, 2018, New tools in CIVA for Model Assisted Probability of Detection (MAPOD) to support NDE reliability studies, ASNT Aerospace Symposium, https://www.extende.com/files/extende/publications/2018_ASNT-Aerospace_Foucher_ToolsinCIVAforReliabilityStudies_EN.pdf

[11]   https://www.extende.com/objectives-of-reliability-in-nde-training

[12]   USA Department of Defense Handbook, 2009, MIL-HDBK-1823-A, NDE system reliability assessment.

[13]   Federal Aviation Administration, "Damage Tolerance for High Energy Turbine Engine Rotors," Advisory Circular 33.14-1, January 8, 2001.